PNAS Nexus, 2023, 2, 1–13
https://doi.org/10.1093/pnasnexus/pgad229
Advance access publication 11 July 2023
Research Report

SUB1A-1 anchors a regulatory cascade for epigenetic and transcriptional controls of submergence tolerance in rice

Chih-Cheng Lin[a,1], Wan-Jia Lee[a,b,1], Cyong-Yu Zeng[a,b], Mei-Yi Chou[a], Ting-Jhen Lin[c], Choun-Sea Lin[a], Meng-Chiao Ho[c,d,*] and Ming-Che Shih[a,b,*]

[a]Agricultural Biotechnology Research Center, Academia Sinica, Taipei 11529, Taiwan
[b]Institute of Plant Biology, National Taiwan University, Taipei 10617, Taiwan
[c]Institute of Biological Chemistry, Academia Sinica, Taipei 11529, Taiwan
[d]Institute of Biochemical Sciences, National Taiwan University, Taipei 10617, Taiwan
*To whom correspondence should be addressed: Email: mcshih@gate.sinica.edu.tw (M.C.S.); joeho@gate.sinica.edu.tw (M.C.H.)
[1]C.-C.L. and W.-J.L. contributed equally to this work.
Edited By: Edward Bayer

Abstract

Most rice (*Oryza sativa*) cultivars cannot survive under prolonged submergence. However, some *O. sativa* ssp. *indica* cultivars, such as FR13A, are highly tolerant owing to the *SUBMERGENCE 1A-1* (*SUB1A-1*) allele, which encodes a Group VII ethylene-responsive factor (ERFVII) protein; other submergence-intolerant cultivars contain a *SUB1A-2* allele. The two alleles differ only by a single substitution at the 186th amino acid position from serine in SUB1A-1 to proline in SUB1A-2 resulting in only SUB1A-1 being able to be phosphorylated. Two other ERFVIIs, *ERF66* and *ERF67*, function downstream of SUB1A-1 to form a regulatory cascade in response to submergence stress. Here, we show that SUB1A-1, but not SUB1A-2, interacts with ADA2b of the ADA2b-GCN5 acetyltransferase complex, in which GCN5 functions as a histone acetyltransferase. Phosphorylation of SUB1A-1 at serine 186 enhances the interaction of SUB1A-1 with ADA2b. *ADA2b* and *GCN5* expression was induced under submergence, suggesting that these two genes might play roles in response to submergence stress. In transient assays, binding of SUB1A-1 to the *ERF67* promoter and *ERF67* transcription were highly induced when SUB1A-1 was expressed together with the ADA2b-GCN5 acetyltransferase complex. Taken together, these results suggest that phospho-SUB1A-1 recruits the ADA2-GCN5 acetyltransferase complex to modify the chromatin structure of the *ERF66/ERF67* promoter regions and activate gene expression, which in turn enhances rice submergence tolerance.

Keywords: submergence, rice, SUB1A-1, ADA2b-GCN5 acetyltransferase complex

Significance Statement

SUBMERGENCE 1A-1(*SUB1A-1*) is a Group VII ethylene-responsive transcription factor (ERFVII) that confers the majority of submergence tolerance to rice. Rice cultivars without *SUB1A-1* or with *SUB1A-2* allele are sensitive to submergence. SUB1A-1 and SUB1A-2 differ by a single amino acid substitution, i.e. Ser186 in SUB1A-1 and Pro186 in SUB1A-2. Under submergence, SUB1A-1 is phosphorylated by MPK3 at Ser186. Previously, we reported that *ERF66* and *ERF67* function downstream of SUB1A-1 to form a regulatory cascade during submergence. This study shows that phosphorylation of SUB1A-1 enhanced its binding to the *ERF67* promoter. In addition, phospho-SUB1A-1 recruits the ADA2-GCN5 to modify the chromatin structure of the *ERF67* promoter region and then activates *ERF67* gene expression.

Introduction

Although rice is cultivated in paddy fields, most cultivars are sensitive to submergence stress and die within several days of complete submergence. However, a few submergence-tolerant rice cultivars, such as FR13A, show extraordinary tolerance. Under complete submergence, the growth of FR13A plant is paused, which is termed "quiescence phenotype." After floods recede, FR13A plants resume growth without lodging as submergence-intolerant rice plants do. *SUBMERGENCE 1A-1* (*SUB1A-1*) is specifically identified in the submergence-tolerant cultivars and plays a determinant role in submergence stress responses (1, 2).

SUB1A-1 is a transcription factor that is classified into the Group VII ethylene-responsive factor (ERFVII) family according to the homology of its singular AP2 domain (1, 2). SUB1A-1 confers the majority of its submergence tolerance by mediating the quiescence response via repression of ethylene and Gibberellin-induced shoot elongation (2–4). Several studies have indicated that SUB1A-1 regulates a spectrum of genes involved in anaerobic metabolism, reactive oxygen species regulation, and leaf

Competing interest: The authors declare no competing interest.
Received: March 1, 2023. **Accepted:** June 28, 2023

senescence during and after submergence (5–8). Most of the ERFVIIs possess a conserved MCGG (Met-Cys-Gly-Gly) motif at the very N-terminal end. The MCGG motif is the N-degron of the oxygen-dependent N-degron pathway of proteolysis. Importantly, the N-degron pathway regulation of ERFVII protein stability was identified as an oxygen-sensing mechanism in Arabidopsis (9, 10). SUB1A-1 possesses the canonical N-degron but is not subjected to the N-degron pathway (9). Two ERFVIIs genes, *ERF66* and *ERF67*, are transcriptionally activated by SUB1A-1 under submergence. The protein stability of ERF66 and ERF67 is regulated by the N-degron pathway in response to low oxygen during submergence. It has been demonstrated that *SUB1A-1* and *ERF66/67* form a regulatory cascade to activate downstream genes for rice submergence tolerance (11).

In addition to *SUB1A-1*, there is another allele, *SUB1A-2*, that is seen only in the submergence-sensitive cultivars, such as IR29. The two alleles contain 17 single nucleotide polymorphisms; there is only one nonsynonymous substitution in the coding region, which results in conversion of the 186th amino acid residue from serine (SUB1A-1) to proline (SUB1A-2) (Fig. S1) (1, 2). This substitution affects the ability of the protein to be phosphorylated. SUB1A-1 has been proposed to be phosphorylated and activated by MITOGEN-ACTIVATED PROTEIN KINASE 3 (MPK3) (12). Although SUB1A-2 was shown to interact weakly with MPK3, it could not be phosphorylated even with increasing concentrations of SUB1A-2. Thus, serine 186 of SUB1A-1 is a specific phosphorylation target site of MPK3. Under submergence, *SUB1A-1* is induced and further regulates the expression of *MPK3* in a positive feedback loop. Hence, MPK3 phosphorylates SUB1A-1 in a SUB1A-1-dependent manner. So far, the differential effects of phosphorylated SUB1A-1 and unphosphorylated SUB1A-2 on submergence tolerance have not been addressed.

Gene expression relies on the physical access of the transcription factor to DNA; therefore, chromatin accessibility is changed in response to changing environmental cues (13). Histone lysine acetylation, which neutralizes a positive charge, often reduces the interaction strength between histone and DNA, resulting in increased chromatin accessibility and is associated with gene transcription activation (14). Histone acetylation is involved in developmental processes and stress resistance, including submergence or hypoxia (15–20).

GENERAL CONTROL NON-REPRESSIBLE 5 (GCN5) is a histone acetyltransferase that associates with ALTERATION/DEFICIENCY IN ACTIVATION 2 (ADA2) to form a histone acetyltransferase module, which is a subcomplex of the Spt-Ada-Gcn5 acetyltransferase (SAGA) coactivator complex (21). ADA2 serves as an adaptor and improves the acetylation activity and substrate specificity of GCN5 (22). Mutations of ADA2 result in disassociation of GCN5 from the SAGA complex and reduction of histone acetylation, gene expression, and cell growth (23). In plants, orthologs of GCN5 and ADA2 have been identified but not well studied (24). T-DNA insertional Arabidopsis mutants of *GCN5* or *ADA2b* show pleiotropic phenotypes, including dwarfism, abnormal root development, floral developmental defect, and abnormal trichome branching (25–27), suggesting that *GCN5* and *ADA2b* are required for proper gene expression. Without sequence-specific DNA recognition properties, the ADA2b-GCN5 module usually associates with sequence-specific transcription factors to regulate downstream gene expression (28, 29).

In rice, the histone acetylation levels of *ADH1* and *PDC1* are elevated under submergence (20). In Arabidopsis, the histone 3 lysine 9 acetylation (H3K9ac) level is increased under hypoxia, particularly in the 49 core hypoxia-responsive genes (19). This suggests that histone acetylation is highly associated with productive transcription under submergence and hypoxia. In this study, we found that the H3K9ac level increased in the *ERF66* and *ERF67* promoters in FR13A under hypoxia. Furthermore, SUB1A-1 is associated with the ADA2b-GCN5 module to transcriptionally activate the expression of *ERF66* and *ERF67*. We also found that phosphorylation of SUB1A-1 enhanced the recruitment of the ADA2b-GCN5 module and increased the expression of *ERF66* and *ERF67*.

Results

SUB1A-1 interacts with ADA2b of the ADA2b-GCN5 acetyltransferase complex

Our previous study showed that SUB1A-1 directly activates *ERF66* and *ERF67* under submergence, resulting in high transcript levels of *ERF66* and *ERF67* (11). It has been reported that SUB1A-1 interacts with several transcription factors that contain a SANT domain (30). The SANT domain–containing protein, ADA2b, is a highly conserved subunit in the SAGA complex and is involved in histone modification (31, 32). To determine whether SUB1A-1 is involved in epigenetic regulation, its ability to interact with ADA2b was tested. When used as a prey in a yeast two-hybrid (Y2H) assay, SUB1A-1, but not SUB1A-2, interacted with ADA2b (Fig. 1A). When used as a bait, SUB1A-1 still interacted with ADA2b (Fig. 1A), ruling out the possibility that SUB1A-1 has self-activation activity. Next, the interactions between SUB1A-1 and GCN5 and between ADA2b and GCN5 were tested. There was an interaction between ADA2b and GCN5 in yeast cells, but no direct interaction was detected between SUB1A-1 and GCN5 (Fig. 1B). This suggested that SUB1A-1 might recruit the ADA2b-GCN5 acetyltransferase complex through ADA2b.

To further confirm the interactions among these three proteins, a multicolor bimolecular fluorescence complementation (BiFC) assay was carried out (33). SUB1A-1, ADA2b, and GCN5 fused with fluorescent proteins were overexpressed in onion epidermal cells. In this assay, N-termini of the fluorescent proteins Venus (nVenus) and Cerulean (nCerulean) are expressed with the C-terminus of cyan fluorescent protein (cCFP). When cCFP interacts with nVenus, yellow fluorescence is produced, whereas when cCFP interacts with nCerulean, blue fluorescence is produced (Fig. 1C). When ADA2b was fused with cCFP and GCN5 and SUB1A-1 were fused with nVenus and nCerulean, respectively, two types of fluorescence emissions were detected, revealing that ADA2b interacts with both SUB1A-1 and GCN5 (Fig. 1C, top panel). In contrast, when GCN5 was fused with cCFP, only yellow fluorescence emission was detected, revealing that GCN5 interacts with ADA2b but not SUB1A-1 (Fig. 1C, second panel). To confirm that the fluorescent proteins did not exhibit self-interaction, empty vectors that contained only the fluorescent proteins (empty nVenus, cCFP, and nCerulean) were expressed as negative controls (Fig. 1C, bottom panel). As shown in the bottom panel of Fig. 1C, no yellow and blue fluorescence emission was detected. In this assay, we coexpressed mCherry-VirD2NLS to indicate the nucleus of cell. These results support the notion that ADA2b physically interacts with both SUB1A-1 and GCN5, specifically in the nucleus, suggesting that it acts as a scaffold protein between SUB1A-1 and GCN5.

Phosphorylation of SUB1A-1 enhances its interaction with ADA2b

To determine whether the difference in the abilities of SUB1A-1 and SUB1A-2 to interact with ADA2b was caused by phosphorylation of SUB1A-1 or a structural difference between SUB1A-1

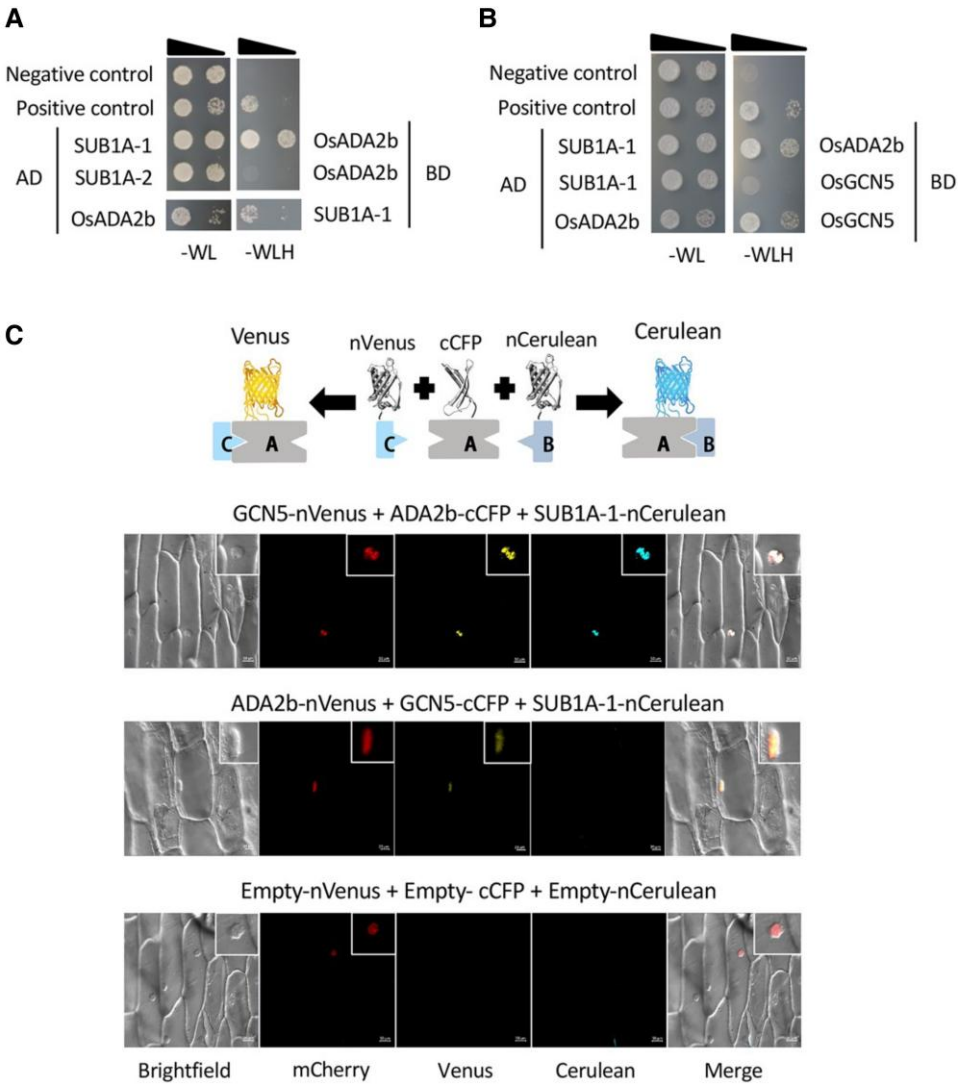

Fig. 1. ADA2b interacts with GCN5 and SUB1A-1, but not SUB1A-2. A) Y2H binding assays of the interaction between SUB1A-1/2 and ADA2b. B) Y2H binding assays of the interaction between SUB1A-1 and ADA2b, SUB1A-1 and GCN5, and ADA2b and GCN5. AD, GAL4 activation domain; BD, GAL4 DNA binding domain. Positive interactions are represented by growth on triple-dropout medium (-WLH), which tests for expression of the *HIS3* reporter gene. Yeast growth on double-dropout medium (-WL) is assessed as a cotransformation control. Ten-fold serial dilutions of yeast cells transformed with the indicated plasmids were grown on -WL and -WLH media. C) Multicolor BiFC binding analysis of the interactions among SUB1A-1, ADA2, and GCN5. In the top panel, onion epidermal cells were cotransformed by particle bombardment with constructs encoding SUB1A-1-nCerulean, ADA2b-cCFP, GCN5-nVenus, and mCherry-VirD2NLS. The mCherry signal indicates the cell nuclei. The Venus signal indicates the interaction of GCN5-nVenus and ADA2b-cCFP. The Cerulean signal indicates the interaction of SUB1A-1-nCerulean and ADA2b-cCFP. In the second panel, GCN5-cCFP was used as the bait and ADA2b-nVenus was used as the prey to perform the swapping test. In the bottom panel, empty-nCerulean, -cCFP, and -nVenus vectors were cotransformed as a negative control. Scale bar, top and bottom panels: 50 μm; second panel: 20 μm.

and SUB1A-2, several mutant alleles were generated and used in Y2H and multicolor BiFC assays. Two phosphorylation-mimicking constructs, *SUB1A-1*^{S186E} and *SUB1A-1*^{S186D}, in which serine 186 of SUB1A-1 was mutated to negatively charged glutamic acid and aspartic acid, respectively, were produced. Moreover, a dephosphorylation-mimicking construct, *SUB1A-1*^{S186R}, in which serine was mutated to positively charged arginine, was produced. Phosphorylation-incompetent SUB1A-1 constructs, *SUB1A-1*^{S186A} and *SUB1A-1*^{S186C}, were produced by mutating serine to alanine and cysteine, respectively. Both Y2H and multicolor BiFC assays showed that *SUB1A-1*^{S186E} was the only mutant form that could interact with ADA2b (Fig. 2). Although *SUB1A-1*^{S186D} is a phospho-mimicking allele, it showed no interaction with ADA2b. Nevertheless, these findings indicated that, rather than a structural difference between SUB1A-1 and SUB1A-2, phosphorylation of SUB1A-1 might be the main reason for the interaction of SUB1A-1, but not SUB1A-2 with ADA2b.

We combined in vitro phosphorylation and pull-down assays to examine the effects of SUB1A-1 phosphorylation on its interaction with ADA2b. To facilitate immunoprecipitation in pull-down assays, SUB1A-1 and ADA2b were tagged with GFP and 2HA, respectively. When coincubated with MPK3 and ATP, SUB1A-1-GFP showed higher binding affinity to 2HA-ADA2b than SUB1A-1-GFP–coincubated MPK3 but without ATP (Figs. 3A and S2). Varying amounts of SUB1A-1-GFP and SUB1A-1^{S186E}-GFP were coincubated with 2HA-ADA2b to determine the effects of SUB1A-1^{186} phosphorylation on interactions between SUB1A-1 and ADA2b. As shown in Fig. 3B, SUB1A-1 interacted with ADA2b when the ratio of SUB1A-1 to ADA2b was 1:1 (i.e. the amounts of SUB1A-1 and ADA2b were both 2 μg). Interestingly,

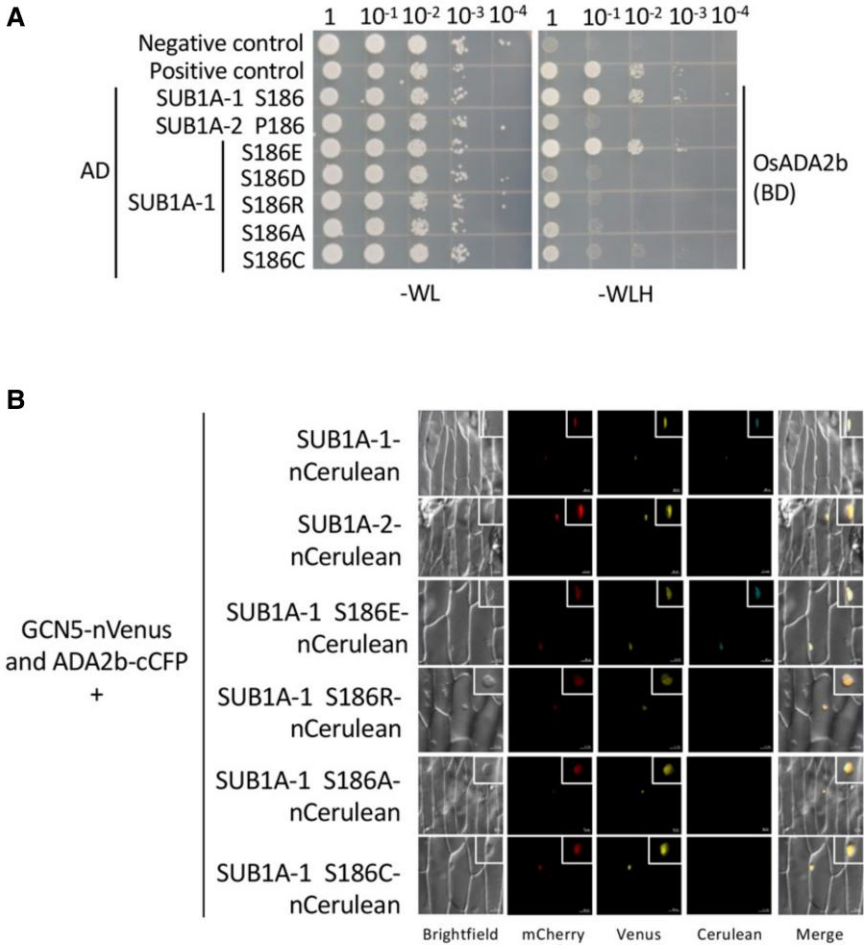

Fig. 2. Phosphorylation of SUB1A-1 is needed for its interaction with ADA2b. A) Y2H binding assays of the interaction between SUB1A-1/2 and SUB1A-1 proteins with various amino acid substitutions (S186E, S186D, S186R, S186A, and S186C) and ADA2b. AD, GAL4 activation domain; BD, GAL4 DNA binding domain. Ten-fold serial dilutions of yeast cells transformed with the indicated plasmids were grown on double-dropout (-WL) medium (cotransformation control) and triple-dropout (-WLH) medium (growth represents a positive interaction). B) Multicolor BiFC binding analysis of the interactions among GCN5, ADA2b, SUB1A-1/2, and SUB1A-1 proteins with various amino acid substitutions (S186E, S186R, S186A, and S186C) in onion epidermal cells. The red fluorescence (from mCherry-VirD2NLS) indicates the cell nuclei. The yellow fluorescence indicates the interaction of GCN5-nVenus and ADA2b-cCFP. The blue fluorescence indicates the interaction of SUB1A-1/SUB1A-1^{S186E}-nCerulean and ADA2b-cCFP. Scale bar, 50 μm.

SUB1A-1^{S186E} bound to ADA2b when the ratio of SUB1A-1^{S186E} to ADA2b was 0.5:1 (i.e. the amount of SUB1A-1 was 1 μg and ADA2b was 2 μg) (Fig. 3B). Although the SUB1A-1/SUB1A-1^{S186E} and ADA2b binding affinities were dosage dependent, SUB1A-1^{S186E} interacted with ADA2b at a lower protein ratio compared with SUB1A-1, suggesting that SUB1A-1^{S186E} has a higher binding affinity to ADA2b.

We then used TNG67 rice protoplasts to perform transactivation assays to determine whether SUB1A-1^{S186E} transcriptionally activates downstream genes. *ERF66* and *ERF67*, which are directly transcriptionally upregulated by SUB1A-1 under submergence, were used as reporter genes. As shown in Fig. 3C, SUB1A-1^{S186E} possessed higher transcriptional activation activity compared with SUB1A-2, but lower activity compared with SUB1A-1. Meanwhile, we used TNG67 rice protoplasts to perform chromatin immunoprecipitation quantitative PCR (ChIP-qPCR) by pulling down GCN5 to analyze the association of the ADA2b-GCN5 module with DNA in the presence or absence of SUB1A-1 and/or MPK3 (Fig. 3D). Coexpression of GCN5, ADA2b, SUB1A-1, and MPK3 showed higher association with the *ERF66* and *ERF67* promoters, suggesting that the ability of the ADA2b-GCN5 module to associate with the *ERF66* and *ERF67* promoters depends on SUB1A-1 and MPK3.

RLR domain in ADA2b is required for the interaction of ADA2b and SUB1A-1

There are three well-known domains within ADA2b, ZnF (ZZ-type zinc-binding) domain, SANT domain, and SWRIM domain (Fig. S3A). In humans, ADA2b interacts with ADA3, which is another component of the SAGA complex, through the N-terminal region of the SANT domain that follows the C-terminal of the SWIRM domain (34, 35). Additionally, ADA2b contacts with GCN5 through the N-terminal of the ZnF domain and the SANT domain (36). It has also been reported that the ADA2b SANT domain affects activation of GCN5 and plays a central role in chromatin remodeling (23, 31, 32). ADA2b is a scaffold protein that brings together GCN5 and transcription factors in plants (16, 18, 28).

A previous study indicated that the conserved central region of ADA2 (named the RLR region) regulates the interaction of ADA2 with phosphoserine proteins (37). The previous study showed that ADA2^{RLR} (R327S, L328A, and R331A) was unable to bind phospholipid proteins in yeast. Referring to the above study, several point mutations in the rice ADA2b^{RLR} region were generated (Fig. S3A). Due to the difference in amino acid sequence of ADA2b between yeast and rice, ADA2b^{SATTA} (R327S, L328A,

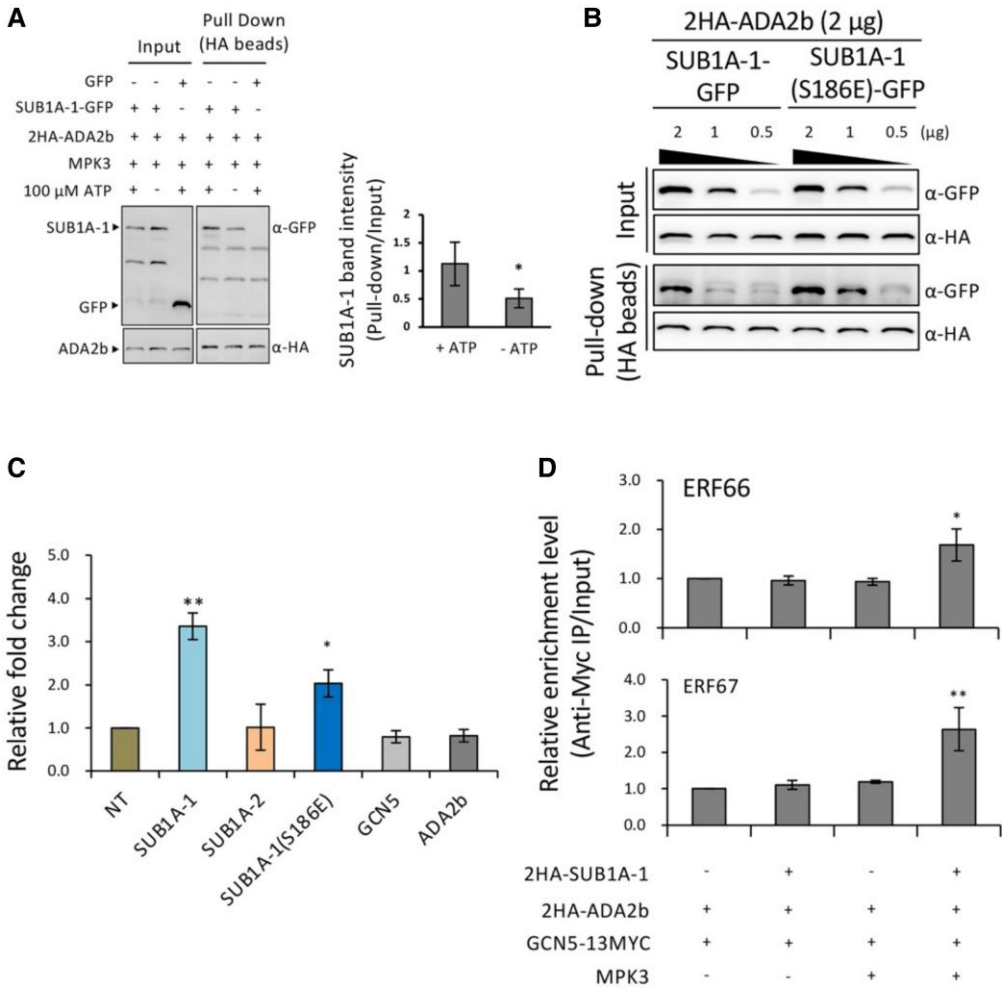

Fig. 3. Phosphorylation of SUB1A-1 enhances its interaction with ADA2b. A) In vitro phosphorylation and pull-down assays testing the effect of SUBA-1 phosphorylation on the interaction between 2HA-ADA2b and SUB1A-1-GFP. Purified recombinant 2HA-ADA2b (2 μg) was first incubated with recombinant SUB1A-1-GFP (2 μg) and MPK3 (~0.2 μg) for 30 min, followed by further incubation with magnetic beads preconjugated with HA antibodies for 1 h. After incubation, beads were washed, eluted, and detected with anti-HA or anti-GFP antibodies. One representative blot is shown of four independent experiments. The bar chart shows quantification of the SUB1A-1-GFP pull-down level relative to the SUB1A-1-GFP input level with or without ATP. The data represent mean ± SD from the four independent experiments. B) In vitro pull-down assay of the interaction between 2HA-ADA2b and SUB1A-1-GFP/SUB1A-1^{S186E}-GFP. Purified recombinant 2HA-ADA2b (2 μg) mixed with serial half-dilutions of recombinant SUB1A-1-GFP or SUB1A-1^{S186E}-GFP (2, 1, and 0.5 μg) was incubated with magnetic beads preconjugated with HA antibodies. After incubation, beads were washed, eluted, and detected with anti-HA or anti-GFP antibody. One representative blot is shown of two independent experiments. C) SUB1A-1 and SUB1A-1 S186E transcriptionally activate the *ERF67* gene. The transcriptional activation assay was conducted by transforming TNG67 protoplasts with SUB1A-1, SUB1A-2, SUB1A-1 (S186E), GCN5, and ADA2b. Total mRNAs were isolated from the transformed protoplasts followed by qRT-PCR analysis of endogenous *ERF67* transcript level. The relative fold change of each experiment was normalized to the nontransformed protoplasts (NT). The data represent mean ± SD from three independent experiments. D) ChIP-qPCR analysis was conducted by transforming TNG67 protoplasts with different combinations of 2HA-SUB1A-1, 2HA-ADA2, MPK3, and GCN5-13MYC. ChIP was performed using magnetic beads preconjugated with MYC antibodies. GCN5 enrichment of the *ERF66* and *ERF67* promoters was analyzed by qPCR. The data represent mean ± SD from the three independent experiments. *P < 0.05 and **P < 0.01, Student's t test.

D329T, E330T, and R331A) was generated to mimic the sequence of the yeast ADA2 mutant. In addition, ADA2b^{RL8A} was produced by mutating the eight charged amino acids (329–336 residues) in ADA2b to alanine.

As shown in Fig. S3B, the deletion of the ZnF domain from ADA2b abolished its interaction with SUB1A-1. Interestingly, the substitution on the ADA2b RLR region affected the ADA2b and SUB1A-1 interaction. ADA2b^{SATTA} and ADA2b^{RL8A} failed to interact with SUB1A-1. These results further confirmed that the RLR region of ADA2b is important for ADA2b to interact with SUB1A-1. To rule out the possibility that the amino acid substitutions caused ADA2b structural changes, the interactions between ADA2b mutant alleles with SUB1A-2 or GCN5 were used to reconfirm the result. SUB1A-2 does not interact with ADA2b. Likewise, deletions of the ZnF domain of ADA2b and ADA2b^{RL8A} showed similar results, in which they failed to interact with SUB1A-2 (Fig. S3C). Moreover, ADA2b^{SATTA} and ADA2b^{RL8A} did not affect the binding of ADA2b with GCN5 (Fig. S3D). Apparently, the amino acid residues 329–336 in the ADA2b RLR region may be a phospho-binding site of ADA2b for SUB1A-1.

GCN5 may play a role under submergence

The transcript levels of *ADA2b* and *GCN5* under submergence were examined in three different rice cultivars, FR13A, IR29, and Swarna. FR13A possesses the submergence-tolerant allele

SUB1A-1, IR29 possesses the submergence-intolerant allele *SUB1A-2*, and Swarna does not possess either allele. Expression of both *ADA2b* and *GCN5* was significantly induced in FR13A after 1 h submergence (Fig. S4). In contrast, *ADA2b* and *GCN5* were not induced in IR29 or Swarna until plants were submerged for 3 h. Although *ADA2b* and *GCN5* expression was enhanced in all three rice cultivars after 6 h of submergence, the expression levels were highest in FR13A.

Next, we examined the global histone acetylation levels of H3K9, K14, K18, and K23 in FR13A, IR29, and Swarna after complete submergence for 24 h. The aerial parts of rice seedlings were harvested before (time 0) and after (time 24) submergence, and the total nuclear proteins were isolated. Immunoblot analyses were performed using antibodies that specifically recognize H3 acetylated at K9, K14, K18, or K23. Compared with time 0, the H3K9ac level in FR13A after 24 h of treatment was slightly but significantly induced (Fig. 4A). By contrast, there was no significant change in H3K9ac levels in IR29 or Swarna. In addition, submergence had no significant effect on H3K14, K18, or K23 acetylation levels in any of the rice cultivars (Fig. S5).

ERF66 and *ERF67* were used to observe the local changes in H3K9ac level. FR13A and IR29 protoplasts were treated with or without sodium sulfite and then subjected to ChIP-qPCR analyses. Sodium sulfite removes dissolved oxygen in aqueous solutions and has been used to induce hypoxia in animals and plants (38–41). After 4 h of treatment with/without sodium sulfite, the transcript levels of hypoxia response marker genes in FR13A and IR29, namely, *ADH2*, *PDC1*, *SUC2*, *SUB1A-1/2*, *ERF66*, and *ERF67*, were induced under sodium sulfite treatment (Fig. S6), indicating that sodium sulfite induced hypoxia in the protoplasts. As shown in Fig. 4B, the histone H3K9ac levels in the *ERF66* and *ERF67* promoters increased under hypoxia in FR13A but were unchanged in IR29. There was no increase in the H3K9ac level of these two promoters when the FR13A protoplasts were cotreated with sodium sulfite and 1-Naphthyl PP1 (NA-PP1, a MPK inhibitor) (Fig. S7). This suggests that phosphorylation of SUB1A-1 is required for the SUB1A-1-mediated transcriptional activation of *ERF66* and *ERF67* which is associated with histone acetylation modification.

To examine the effects of GCN5 on submergence tolerance, 14-day-old FR13A seedlings were pretreated with γ-butyrolactone (MB-3) (42), which specifically inhibits the catalytic activity of GCN5. FR13A seedlings were pretreated with or without MB-3 for 24 h and then subjected to submergence treatment at 28°C with a 16 h light/8 h dark cycle for 14 days. In previous studies, Arabidopsis seedlings grown in 100 μM MB-3 showed a yellow leaf phenotype, along with a reduction of H3K9 and H3K14 acetylation levels (43, 44). Similarly, FR13A pretreated with MB-3 showed a more severe yellow shoot phenotype compared with control (DMSO-treated) plants after submergence treatment (Fig. 4C), indicating that loss of GCN5 function may increase the submergence sensitivity of FR13A. The phenotypic experiment indicated that GCN5 might be involved in FR13A response to submergence, probably by regulating the histone acetylation levels of submergence-related genes.

SUB1A-1 interacts with the ADA2b-GCN5 acetyltransferase complex to enhance *ERF66* and *ERF67* expression

We have shown previously that the recombinant SUB1A-1 protein could interact with GCC1 boxes in the *ERF66* and *ERF67* promoters (ERF66-GCC1, ERF67-GCC1) but not with the SUB1A-1-GCC1 in EMSA assays (11). Using the same experimental setup, we found that SUB1A-2 binds equally as well as SUB1A-1 to the GCC1 boxes of *ERF66* and *ERF67* in vitro (Fig. 5A). To determine whether the phosphorylation state of SUB1A-1 or SUB1A-2 affects the in vivo binding of these two proteins to the promoter regions of *ERF66* and *ERF67*, we performed ChIP-qPCR in TNG67 rice protoplast to analyze the association of SUB1A-1 and SUB1A-2 with these promoters in the presence or absence of MPK3. In the absence of MPK3, there were no significant differences between the binding affinities of SUB1A-1 and SUB1A-2 for the *ERF66* and *ERF67* promoters (Fig. 5B). In the presence of MPK3, SUB1A-1 bound the *ERF66* and *ERF67* promoters with significantly higher efficiency than SUB1A-2. NA-PP1 reduced the SUB1A-1–specific enrichment on the *ERF66* and *ERF67* promoters in the presence of MPK3 (Fig. 5B). These results indicated that phosphorylation of SUB1A-1 enhanced its binding to the *ERF66* and *ERF67* promoters in vivo. In addition, phosphorylation of SUB1A-1 is required for binding to ADA2b. Consequently, during transcription, phospho-SUB1A-1 might form a stable protein complex with the ADA2b-GCN5 module sitting on the promoter of *ERF66/67* for transcriptional activation. This might be the reason why we could see the higher occupancy of SUB1A-1 in the presence of MPK3.

We next examined the effects of the ADA2b-GCN5 module on transcriptional activation of *ERF66* and *ERF67* by SUB1A-1. We used TNG67 rice seedlings, which possess neither *SUB1A-1* nor *SUB1A-2*, to prepare the protoplasts and the transcript levels of the endogenous *ERF66* and *ERF67* genes as the reporters. Consistent with our previous report (11), SUB1A-1 could activate *ERF66* and *ERF67* (Fig. 5C). As shown in Fig. 5C, individually expressed ADA2b and GCN5 did not transcriptionally activate *ERF66* and *ERF67*. Interestingly, coexpression of SUB1A-1, ADA2b, and/or GCN5 resulted in higher activation of *ERF66* and *ERF67* compared with singly expressed SUB1A-1. It is noteworthy that overexpression of SUB1A-2 alone or coexpressed with ADA2b and/or GCN5 could not enhance the transcriptional activation of *ERF66* and *ERF67*. This provides strong evidence that, although SUB1A-1 and SUB1A-2 could both bind to GCC boxes of *ERF66* and *ERF67*, phosphorylation of serine 186 of SUB1A-1 can enhance the interaction of SUB1A-1 with the ADA2b-GCN5 acetyltransferase complex, which transforms the chromatin of *ERF66* and *ERF67* to an open state, thereby inducing transcription in response to submergence stress.

Discussion

In rice, *SUB1A-1* is a key regulator of the quiescence submergence-survival response (1, 2). It is also known that a single amino acid substitution in SUB1A-1 resulting in SUB1A-2 cannot be phosphorylated by MPK3 and shows poor submergence induction (1, 11, 12). What has not been clear is the reason that cultivars carrying different alleles respond differently to submergence. This study tries to fill in the gap, allowing further understanding of the SUB1A-1 regulatory cascade responses to submergence stress in rice. Here, we reported an epigenetic regulation involving the coordination of the ADA2b-GCN5 acetyltransferase complex and SUB1A-1 for activating SUB1A-1–regulated genes, *ERF66* and *ERF67*, and enhancing submergence tolerance in rice (Fig. S8).

ADA2b is one component of the ADA2b-GCN5 acetyltransferase complex. In yeast, ADA2 serves as a transcriptional adaptor to associate with GCN5 (23). In vitro assay showed that GCN5 catalytic activity was potentiated by associating with ADA2 (22). Mutation on ADA2 in yeast resulted in disassociation of GCN5 from the SAGA complex, and reduction of gene expression and cell growth (23). The Y2H analyses showed that there was an

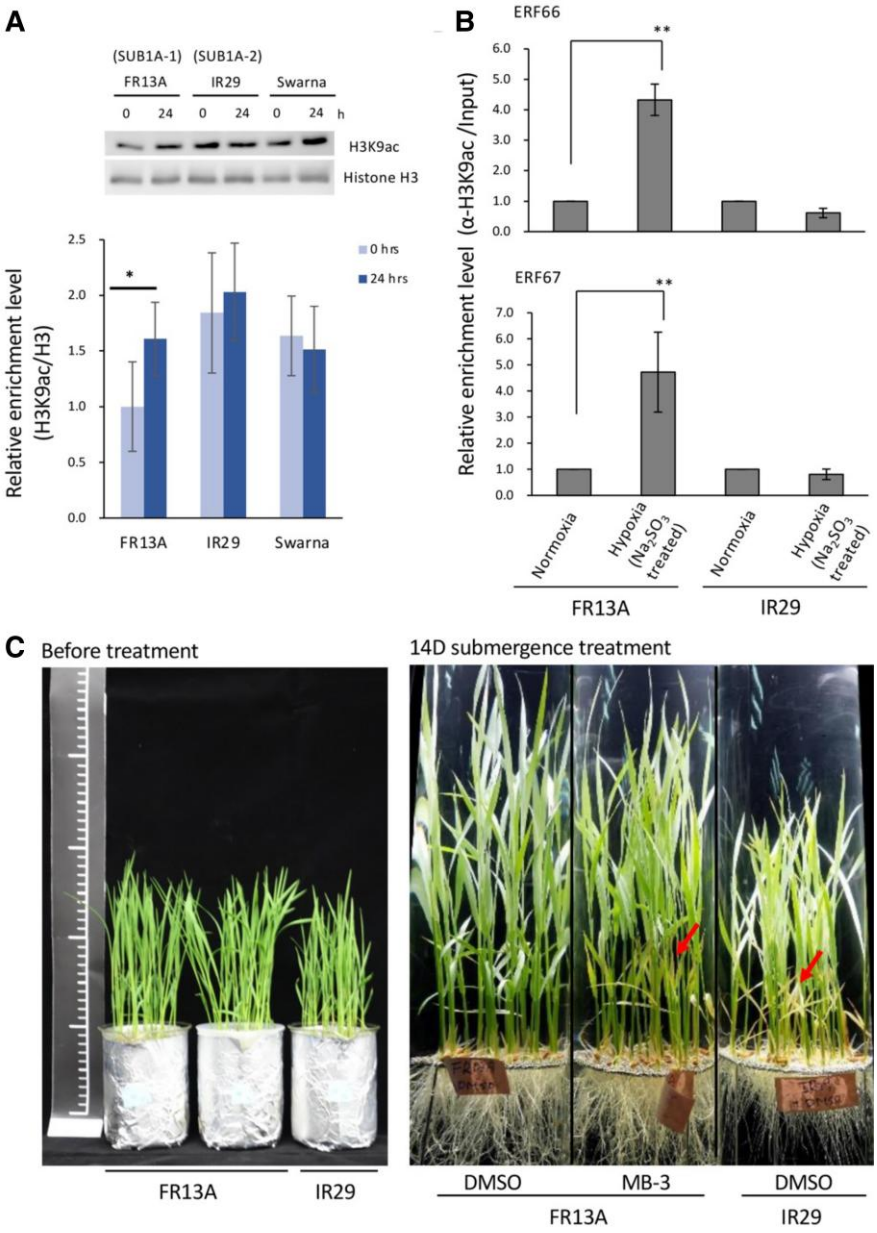

Fig. 4. The level of histone acetylation changes during submergence. A) Global level of H3K9ac in FR13A, IR29, and Swarna rice seedlings before and after submergence treatment. Fourteen-day-old rice seedlings were sampled before and after 24 h of submergence treatment. One representative blot of three independent experiments is shown. The bar chart shows quantification of the H3K9ac levels compared with the H3 levels under each condition. The data represent mean ± SD from the three independent experiments. *$P < 0.05$, Student's *t* test. B) Analysis of H3K9ac enrichment in the *ERF66* and *ERF67* promoters using ChIP-qPCR. The FR13A and IR29 rice protoplasts were treated with 0.5 g/L Na_2SO_3 for 4 h in the dark, and the normoxic control was incubated in W5 buffer in parallel. The data represent mean ± SD from four independent experiments. **$P < 0.01$, Student's *t* test. C) Phenotypes of FR13A treated with MB-3 or DMSO (negative control) and IR29 after 14 days of submergence. Fourteen-day-old FR13A seedlings were pretreated for 1 day with 100 μM MB-3 or DMSO and submerged for 14 days. IR29 seedlings were used as a submergence-intolerant control. Images were taken before and 14 days after submergence.

interaction between rice ADA2b and GCN5 (Fig. 1B). Meanwhile, there was no direct interaction between SUB1A-1 and GCN5 (Fig. 1B). The multicolor BiFC analyses also showed similar results in onion epidermal cells (Fig. 1C, second panel). GCN5-cCFP fusion protein can interact with ADA2b-nVenus fusion protein to generate the yellow fluorescence. However, there was no blue fluorescence observed, indicating that there was no interaction between GCN5-cCFP and SUB1A-1-nCerulean.

We found that SUB1A-1 interacts with ADA2b in yeast cells (Fig. 1A). As shown in the top panel of Fig. 1C, ADA2b-cCFP fusion protein interacted with GCN5-nVenus fusion protein to generate the yellow fluorescence and ADA2b-cCFP fusion protein interacted with SUB1A-1-nCerulean fusion protein to generate the blue fluorescence. It is therefore suggested that SUB1A-1 is associated with the ADA2b-GCN5 acetyltransferase complex via interacting with ADA2b.

There is a noticeable difference in the binding affinities of SUB1A-1/2 to ADA2b (Fig. 1A). To determine whether the difference was caused by phosphorylation of SUB1A-1, we conducted Y2H and multicolor BiFC with a series of mutant alleles. As shown in Fig. 2, SUB1A-1 and the S186E mutant allele could interact with ADA2b but SUB1A-2 could not. Although there is no report on the

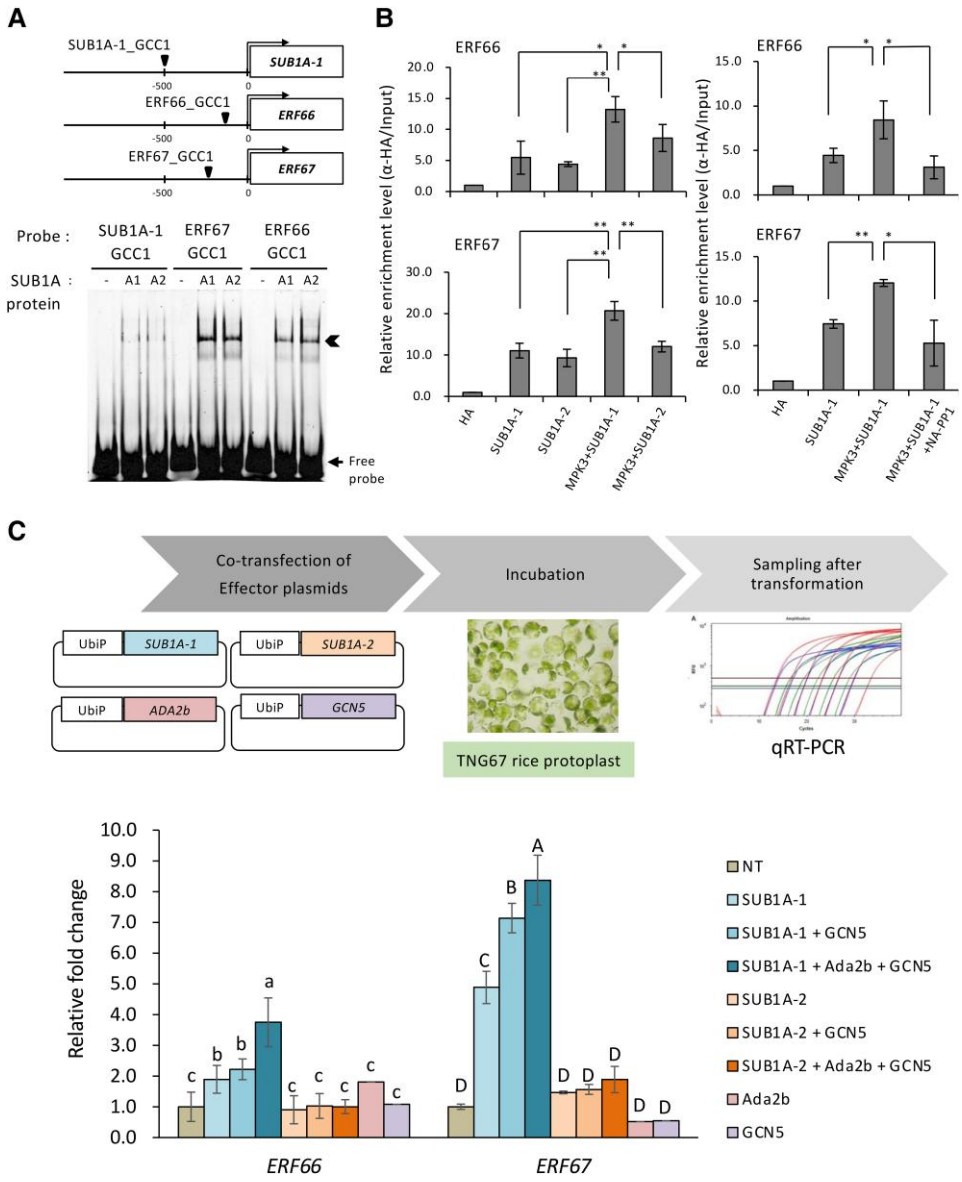

Fig. 5. SUB1A-1 cooperates with the ADA2b-GCN5 module to activate *ERF66* and *ERF67* gene transcription via elevation of histone acetylation modification. A) EMSA assays of the interaction between recombinant SUB1A-1 (A1) and SUB1A-2 (A2) and FAM-labeled DNA probes containing the GCC1 box from *SUB1A*, *ERF66*, and *ERF67* promoters. B) ChIP-qPCR assays of SUB1A-1 and SUB1A-2 interactions with the *ERF66* and *ERF67* promoters in vivo. SUB1A-2 was associated with the *ERF66* and *ERF67* promoters, but SUB1A-1 showed specific enrichment on the *ERF66* and *ERF67* promoters in the presence of MPK3. NA-PP1, a MPK inhibitor, reduced the SUB1A-1–specific enrichment on the *ERF66* and *ERF67* promoters in the presence of MPK3. The data represent mean ± SD from the three independent experiments. $^{*}P < 0.05$ and $^{**}P < 0.01$, Student's *t* test. C) Assay of transcriptional activation of the *ERF66* and *ERF67* genes by SUB1A-1 and the ADA2-GCN5 module. TNG67 rice protoplasts were cotransformed with SUB1A-1/2, ADA2b, and/or GCN5; then, total mRNAs were isolated followed by qRT-PCR analysis of endogenous *ERF66* and *ERF67* transcript levels. The relative fold change of each experiment was normalized to the nontransformed protoplasts (NT). The data represent mean ± SD from three independent experiments. Different letters indicate significant differences among treatments as determined by LSD test.

existence of MPK3 homolog in yeast, several mitogen-activated protein kinases (MAP kinases), such as Fus3, have been reported (45–47). Since SUB1A-1 possesses a similar canonical MAPK phosphorylation sequence (1, 45), yeast MAP kinase may contribute to some level of SUB1A-1 phosphorylation, resulting in ADA2b interaction shown in Y2H. The phosphorylation-incompetent mimics, S186C or S186A, showed no ADA2b interaction, which supports our hypothesis. In addition, multicolor BiFC in the plant system also showed the same results (Fig. 2B).

We also showed that phosphorylation of SUB1A-1 at Ser^{186} enhances its interaction with ADA2b of the ADA2b-GCN5 acetyltransferase complex (Figs. 3A and B and S2), leading to the enhanced expression of *ERF66* and *ERF67* during submergence (Fig. 3C). In Fig. 3B, the S186E variant showed higher binding affinity to ADA2b. Since in the binding reactions, SUB1A-1 was not phosphorylated, it showed a relatively weak binding affinity to ADA2b. Phosphoserine possesses a moiety with two negative charges, while glutamate possesses a moiety with only one negative charge which is sterically smaller to that of phosphoserine. Substitution of glutamate for phosphoserine might show similar but not the same level of activation activity (48, 49). In Fig. 3C, SUB1A-1 S186E protein possessed higher transcription activation activity compared with that of SUB1A-2. However, the glutamate substitution is an imperfect mimic of serine phosphorylation (48)

resulting in a weaker activation compared with the SUB1A-1. The occupancy of GCN5 on the promoters is increased in the presence of SUB1A-1 and MPK3 (Fig. 3D), suggesting that phospho-SUB1A-1 recruits the ADA2b-GCN5 module to enhance *ERF66* and *ERF67* expression.

We further showed that phospho-SUB1A-1 has a strong interaction with the ADA2b-GCN5 acetyltransferase complex particularly through the recruitment of the ADA2b RLR region (Fig. S3). Previous studies have shown that a conserved central region within yeast ADA2 is important for its protein stability and transcription activation of downstream genes (23, 50). The current study has shown that this central region interacts with phosphatidylserine which contains part phosphoserine and phosphatidylserine binding of ADA2 is highly correlated to the functions of ADA2 (37). Phosphatidylserine contains a serine attached through a phosphodiester linkage which is like a phosphoserine. We mutated this conserved central region of rice ADA2b and found the mutation on this region abolished ADA2b binding to SUB1A-1 but not GCN5.

The cooperation of the ADA2b-GCN5 acetyltransferase complex with SUB1A-1 promoted transcription of *ERF66* and *ERF67* (Fig. 5). Likewise, coexpression of the ABA-responsive transcription factor, AREB1, and ADA2b-GCN5 acetyltransferase complex in *Populus trichocarpa* protoplasts highly induced downstream drought-regulated genes (18). In fact, we found that the transcription efficiency of *ERF67* showed a similar pattern when SUB1A-1 and GCN5 were overexpressed with or without ADA2b (Fig. 5). This may be due to the characteristics of ADA2b among the SAGA complex, which acts as a scaffold for the HAT module to interact with transcription factors (18, 28, 51). Thus, the endogenous ADA2b may be sufficient for this mechanism in rice, resulting in no significant difference when ADA2b was overexpressed.

One way that histone acetylation contributes to transcriptional activation is by increasing the chromatin accessibility. Acetylation of lysine residues in the histone N-terminal tail reduces the binding strength of the histone to DNA, which leads to an open chromatin structure and results in an increase in chromatin accessibility to transcriptional machinery proteins, including transcription factors (52). In plants, an increased histone acetylation level is correlated with developmental and cellular processes (16, 17, 53) and several abiotic stresses, such as drought, cold, submergence, and hypoxia (15, 18–20). In *P. trichocarpa*, H3K9 acetylation was reported as an important marker of gene activation in response to drought stress (18). Hypoxia-responsive genes in rice, such as *ADH1* and *PDC1*, were found to have higher total acetylation levels at H3K9 and K14 under submergence conditions compared with aerobic conditions (20). In Arabidopsis, the 49 core hypoxia-responsive genes are transcribed rapidly in response to hypoxia, which is accompanied by higher H3K4me3 and H3K9ac levels and a higher rate of H2A.Z eviction on these genes, suggesting that epigenetic regulation is important for gene expression in response to abiotic stresses (19). Similarly, we observed that the local histone acetylation levels of H3K9 on *ERF66* and *ERF67* in FR13A increased under submergence (Figs. 4B and S7). Under submergence stress, H3K9ac was used to mark the selected stress-related genes; therefore, only submergence-responsive genes were transcribed to conserve energy usage. Inhibition of GCN5 catalytic function affected the survivability of FR13A under submergence stress (Fig. 4C). This suggests that GCN5 may mediate the recruitment of H3K9ac to the promoter of *ERF66* and *ERF67*, inducing a permissive chromatin structure for elevated gene expression leading to enhancement of FR13A tolerance to submergence stress.

Materials and methods

Plant materials, growth conditions, and submergence treatment

Rice (*Oryza sativa*) cultivar FR13A, IR29, Swarna, and Tainung67 (TNG67) were used in this study. Rice seeds were sterilized with 1.2% (v/v) sodium hypochlorite containing 0.1% (v/v) Tween 20 for 30 min and washed with sterilized water at least five times. The sterilized seeds were placed in petri dishes with moist filter paper, followed by incubation at 37°C in the dark for 4 days. Next, uniformly germinated seeds were transplanted onto an iron grid in a beaker containing Kimura B solution (quarter strength, pH 5.6–5.8) and the Kimura B solution was renewed every two days. The cultivated seedlings were cultured in a growth chamber at 28°C under a 16-h-light (120–125 μmol·m^{-2}·S^{-1})/8-h-dark cycle for another 6 to 10 days. Submergence treatments were conducted as described previously (11). For γ-butyrolactone (MB-3, M2449, Sigma-Aldrich) treatment (42), individual plants were pretreated with 100 μM MB-3 or DMSO (mock control) for 24 h before submergence treatment. Next, the plants were transferred into a 3-L water tank (W:L:H, 10 × 10 × 50 cm) filled with water to a height of 40 cm for phenotypic observation.

Yeast two-hybrid assay

The yeast two-hybrid (Y2H) assays were performed using the GAL4-based yeast two-hybrid system (Matchmaker Gold Yeast Two-Hybrid System, Clontech). Full-length coding sequences (CDSs) of *SUB1A-1*, *SUB1A-1* single amino acid substitution mutants (including S186E, S186D, S186R, S186A, and S186C), *SUB1A-2*, *ADA2b* (LOC_Os03g55450), and *GCN5* (LOC_Os10g28040) were cloned into the pGADT7-DEST and pGBKT7-DEST using the Gateway system (Invitrogen). The pGADT7-AKIN10 (At3g01090.1) and pGBKT7-At5g20700 plasmids were used as positive bait and prey controls. The pGADT7-T and pGBKT7-Lam plasmids were used as negative bait and prey controls. SD-WL (-Trp, -Leu) medium was used to select for the presence of both bait and prey vectors, and SD-WLH (-Trp, -Leu, and -His) medium was used to check the interaction between the bait and prey proteins.

Particle bombardment

Particle bombardment was conducted as described previously (11) using Biolistic Particle Delivery System (Bio-Rad) PDS-1000. The upper epidermal layer of the onion was peeled and placed on a plate containing half-strength MS medium (0.25% sucrose). A total of 3.5 μg of each plasmid DNA was used, and the gold particles size was 1.0 μm (Inbio Gold). There were a total of 0.3–0.4-mg particles per shot, and the particles were accelerated with a pressure of 1,100 psi. The distance from the projectile source to the sample was 6 cm. After bombardment, the onion epidermal layers were incubated at room temperature in the dark for 16 h before observation.

Multicolor biomolecular fluorescence complementation

The multicolor biomolecular fluorescence complementation (BiFC) assays were conducted as described previously (33). The bait protein was fused with the C-terminus of CFP (cCFP), and prey proteins were fused with the nVenus or nCerulean. The interaction of nVenus-tagged protein and cCFP-tagged protein generates yellow fluorescence, and the interaction of nCerulean-tagged protein and cCFP-tagged protein generates blue fluorescence. pSAT1A-nVenus-C (pE3288, ABRC stock number: CD3–1026), pSAT1A-nCerulean-C (pE3415, ABRC stock number: CD3-1072), and pSAT1A-cCFP-N

(pE3450, ABRC stock number: CD3-1063) were obtained from ABRC, Ohio State University. Full-length CDSs of *GCN5* and *ADA2b* were cloned into pSAT1A-nVenus-C and pSAT1A-cCFP-N, respectively. Full-length CDSs of *SUB1A-1*, *SUB1A-1* single amino acid–substituted mutants (namely, S186E, S186R, S186A, and S186C), and *SUB1A-2* were cloned into pSAT1A-nCerulean-C. pSAT1A-nVenus-C, pSAT1A-nCerulean-C, and pSAT1A-cCFP-N were used as the empty vector controls. pSAT6-mCherry-VirD2NLS, which generate red fluorescence, was used to indicate the transfected cells and subcellular structures. pSAT6-mCherry-VirD2NLS was obtained from Professor Stanton Gelvin, Purdue University. The plasmids for expressing SUB1A-1, ADA2b, and GCN5 together with mCherry-VirD2NLS were cotransfected into onion epidermal cells by particle bombardment. Fluorescence was detected by an LSM 780 plus ELYRA confocal microscope. The objective lens was a Plan-Apochromat 10×/0.45. Channel specifications were as follows: (i) Venus track: Argon laser, 514 nm; (ii) Cerulean track: Diode 440-16, 440 nm; and (iii) mCherry track: DPSS 561-10, 561 nm.

Protein expression and purification

To express the tag-fused recombinant SUB1A-1, SUB1A-1^{S186E}, ADA2b, and MPK3 proteins, full-length CDS of SUB1A-1, SUB1A-1^{S186E}, GFP, and 2HA-ADA2b fragment (which was amplificated from pUbiP-2HA-ADA2b-NosT) were cloned into pET32a (removal of the Trx and S tags was by PCR amplification using the back-to-back positions of the forward and reverse primers which are located outside the nucleic acid sequence of the Trx and S tags) using the NEBuilder HiFi DNA Assembly Cloning Kit (M5520, NEB) to generate the pET32a-SUB1A-1-GFP-6His and pET32a-SUB1A-1^{S186E}-GFP-6His, pET32a-GFP-6His, and pET32a-2HA-ADA2b-6His plasmids, respectively. The pET32a-Trx-S-MPK3-6His was generated by Gibson assembly of the MPK3 CDS and pET32a. These plasmids were transformed into *Escherichia coli* Roseta (DE3) for recombinant protein production. The transformed cells were cultured in a LB medium containing 100 μg/mL ampicillin at 37°C; then, the cells were induced at an optical density of 1 by adding 1 mM IPTG at 16°C for 16 h. After centrifugation, the harvested cells were resuspended in lysis buffer (1× PBS at pH 7.4 plus with 10 mM imidazole, 1 mM PMSF, and DNase) and then lysed by sonication. After centrifugation at 20,000*g* and 4°C for 20 min, the supernatant was loaded onto a column containing NiNTA resin pre-equilibrated with lysis buffer. The column was washed with 10 column volumes of wash buffer I (1× PBS at pH 7.4 plus with 20 mM imidazole), then with 10 column volumes of wash buffer II (1× PBS at pH 7.4 plus with 50 mM imidazole) in order. Proteins were eluted with elution buffer (1× PBS at pH 7.4 plus 500 mM imidazole).

In vitro phosphorylation and pull-down assay

The in vitro phosphorylation assays were conducted as described previously with minor modifications (54). Recombinant SUB1A-1-GFP (2 μg) or GFP only (2 μg) were coincubated with 2HA-ADA2b (2 μg) and MPK3 proteins (0.2 μg) in a reaction buffer (20 mM HEPES at pH7.4, 150 mM NaCl, 10 mM $MgCl_2$) supplied with 100 μM ATP or not. The total volume of each reaction mixture was 500 μL. The reaction mixtures were gently mixed at room temperature on a rotor, 12 rpm for 30 min, and 10% of each mixture was set aside as input. Next, each mixture was supplemented with 20 μL anti-HA magnetic beads (88836, Pierce) which were pre-equilibrated with 1× PBS at pH 7.4 plus with 0.2% BSA and mixed on a rotor 1 h. Beads were washed three times with reaction buffer, followed by elution in reaction buffer plus with 5× SDS sample buffer at 95°C for 5 min. After 10% SDS-PAGE separation followed by electroblotting, the SUB1A-1-GFP/GFP only and 2HA-ADA2b proteins were detected with anti-GFP and anti-HA antibodies, respectively.

In vitro pull-down assay

The in vitro pull-down assays were conducted as described previously with minor modifications (55). Recombinant 2HA-ADA2b (2 μg) was coincubated with SUB1A-1-GFP or SUB1A-1^{S186E}-GFP at three different mass ratios (1:1, 1:0.5, and 1:0.25) in binding buffer (25 mM Tris-HCl at pH 8, 300 mM NaCl, 0.1% NP-40, 0.1 mg/mL BSA, 1 mM PMSF, and protease inhibitor cocktail) in a total volume of 500 μL. The reaction mixtures were gently mixed at 4°C on a rotor, 12 rpm for 10–15 min, and 3% of each mixture was set aside as input. Next, each mixture was supplemented with 20 μL anti-HA magnetic beads which were pre-equilibrated with binding buffer and mixed on a rotor for another 6 h. Beads were washed three times with binding buffer, followed by elution in 1.5× SDS sample buffer at 95°C for 5 min. After 10% SDS-PAGE separation followed by electroblotting, the SUB1A-1-GFP/SUB1A-1^{S186E}-GFP, and 2HA-ADA2b proteins were detected with anti-GFP and anti-HA antibodies, respectively.

Histone extraction

The histone extraction was conducted as described previously with minor modifications (56). One gram of shoot tissues of rice seedling was collected and ground into fine powder with liquid nitrogen. The powder samples were resuspended in 30 mL of cold extraction buffer 1 (0.4 M sucrose, 10 mM Tris-HCl; pH 8.0, 10 mM $MgCl_2$, 10 mM sodium butyrate, 5 mM β-ME, 0.1 mM PMSF, and protease inhibitor cocktail). After ice bathing for 5 min, the extraction mixture was filtered through a 40-μm cell strainer (352340, Falcon). The filtrate was centrifuged at 3,000*g*, 4°C for 20 min. After centrifugation, the supernatant was removed and the pellet was resuspended in 1 mL of cold extraction buffer 2 (0.25 M sucrose, 10 mM Tris-HCl; pH 8.0, 10 mM $MgCl_2$, 5 mM β-ME,0.1% Triton X-100, 0.1 mM PMSF, and protease inhibitor cocktail). The resuspended mixture was centrifuged at 12,000*g*, 4°C for 10 min to collect the cell nuclei. After centrifugation, the supernatant was removed and the pellet was resuspended in 300 μL of nuclei lysis buffer (50 mM Tirs-HCl; pH 8.0, 10 mM EDTA, 1% SDS, and protease inhibitor cocktail). The cell nuclei were lysed by repeated freezing with liquid nitrogen and thawing in a 37°C water bath three times. The lysate was centrifuged at 12,000*g* and 4°C for 5 min, and then, the supernatant containing histone protein was transferred into a new tube. After 12% SDS-PAGE separation followed by electroblotting, the histone 3 proteins were detected with anti-H3, H3K9ac, H3K14ac, H3K18ac, and H3K23ac antibodies, respectively.

Western blot analysis and antibodies

The protein extraction was conducted as described previously (11). Proteins resolved by SDS-PAGE were transferred to PVDF using a MiniTrans-Blot electrophoretic transfer cell (Bio-Rad). Membranes were probed with primary antibodies at the following titers: anti-H3 (AS10710, Agrisera; 1:20,000), anti-H3K9ac (07-352, Sigma-Aldrich; 1:2,500), anti-H3K14ac (07-353, Sigma-Aldrich; 1:2,500), anti-H3K18ac (07-354, Sigma-Aldrich; 1:2,500), anti-H3K23Ac (07-355, Sigma-Aldrich; 1:2,500), anti-HA (H3663, Sigma-Aldrich, 1:1000), and anti-GFP (11814460001, Roche, 1:3000). HRP-conjugated anti-mouse (NEF822001EA, PerkinElmer)/rabbit (DC03L, Calbiochem) secondary antibody was used at a titer of 1:3,000. Immunoblots were

visualized with enhanced chemiluminescence reagent (SuperSignal West Pico/Dura, Thermo Scientific). The relative image intensities were quantified by ImageJ (https://imagej.nih.gov/ij/).

Chromatin immunoprecipitation quantitative PCR

The ChIP-qPCR assays were conducted as described (11). Briefly, after transformation and 4-h of incubation, the transformed protoplasts (1.6×10^6 cells per transformation) were collected by centrifugation at 200*g* for 2 min. After removing the supernatants, the collected protoplasts were subjected to cross-linking with 1% formaldehyde in 1.5 mL W5 solution and gently mixed at room temperature on a rotor (Intelli Mixer ERM-2L, ELMI) at 12 rpm for 10 min. To quench the cross-linking reaction, 80 μL of 2M glycine was added and the sample was mixed on a rotor for another 5 min. After centrifugation and removal of supernatant, the protoplasts were rinsed with 1 mL of ice-cold 1× PBS (137 mM NaCl, 2.7 mM KCl, 10 mM Na_2HPO_4, and 1.8 mM KH_2PO_4). Chromatin extraction, MNase digestion, sonication, immunoprecipitation, reverse cross-linking, DNA recovery, and qPCR were performed by using the Pierce Magnetic ChIP kit (26157, Thermo Scientific) according to the manufacturer's instructions. A total of 5 μg of anti-H3K9ac antibody (C15210015, Diagenode) was used for each IP. The bound DNA fragments were then reversed DNA cross-linked and eluted, followed by qPCR with the specific primers. The full-length MPK3 CDS was cloned into the pUC18-UbiP-NosT vector to generate the pUC18-UbiP-MPK3-NosT plasmid. To observe the occupancy of SUB1A-1 on the *ERF66/67* promoters, the pUbiP-2HA-SUB1A-1-NosT and/or pUC18-UbiP-MPK3-NosT plasmids were used for protoplast transformation. Anti-MYC magnetic beads (88843, Pierce) and anti-HA magnetic beads (88836, Pierce) were used for protein pull-down. The sodium sulfite (Na_2SO_3) used for hypoxia treatment was 0.5 g/L (38). The working concentration of NA-PP1 (1-Naphthyl PP1, ab1506, Abcam) is 10 μM (57). The primers used in ChIP-qPCR are listed in Table S1.

Protoplast preparation and transformation

Rice protoplast preparation and transformation were conducted as described previously (11). Briefly, the 11- to 14-day-old TNG67 rice seedlings were used for protoplast preparation. The stem and sheath of rice seedlings were diced and incubated in an enzyme solution (2% Cellulase RS [Yakult], 1% Macerozyme R10 [Yakult], 0.1% MES at pH 5.6, 0.6 M mannitol, 0.1% $CaCl_2$ and 1% BSA) for 3.5 h. The digestion mixture was filtered through a 40-μm cell strainer and then centrifuged at 200*g* for 3 min to pellet the protoplasts. Then, the protoplasts were washed with W5 solution (154 mM NaCl, 125 mM $CaCl_2$, 5 mM KCl, 5 mM glucose, and 2 mM MES at pH5.7) twice. About 4×10^5 protoplasts were used for transformation. After transformation, the protoplasts were incubated in the dark at room temperature for further analyses.

Transcription activation assay

To test the effect of SUB1A-1/2, ADA2b, and GCN5 on endogenous *ERF66* and *ERF67* gene expression, the rice protoplast system was adopted. The CDSs of *SUB1A-1/2* and *ADA2b* were cloned into pUbiP-2HA-ccdB-NosT, the CDS of *GCN5* was cloned into pGWB520, and the CDS of *MPK3* was cloned into pUBiP-ccdB-NosT using the Gateway system. TNG67 rice protoplasts were cotransformed with SUB1A-1, ADA2b, and GCN5 in various combinations (10 μg of each construct in each experiment) as shown in Figs. 3C and 5C. After transformation, the protoplasts were incubated for 4 h in the dark at room temperature. Protoplast samples were collected by centrifugation followed by RNA extraction and qRT-PCR analyses.

RNA extraction and qRT-PCR

Total RNA was isolated from the treated samples using TRIzol (Invitrogen) following the manufacturer's instructions. DNase treatment, reverse transcription, and qRT-PCR were conducted as described previously (11). Briefly, 0.5 μg total RNA from shoot tissues and 0.1 μg total RNA from protoplasts were used as template for the first-strand cDNA synthesis by M-MLV reverse transcriptase (Invitrogen). The synthesized cDNAs were 5-times diluted. qRT-PCR was conducted using 1 μL diluted cDNA, 0.2 μM each primer, and SYBR Green PCR Master Mix (Applied Biosystems) on an ABI 7500 real-time PCR system using the default settings (Applied Biosystems). Tubulin (LOC_Os07g38730) was used as the reference gene for normalization. The primer sequences are listed in Table S1.

Electrophoretic mobility shift assay

The electrophoretic mobility shift assays (EMSAs) were conducted as described previously (11). Briefly, fluorescein amidite (FAM)–labeled DNA probes were synthesized by Purigo Biotechnology. Each DNA–protein binding reaction mixture contained 0.05 μM FAM-labeled probe, 0.5 μM recombinant proteins, 17 mM HEPES at pH 7.9, 60 mM KCl, 7.5 mM $MgCl_2$, 0.12 mM EDTA, 17% glycerol, 1.2 mM dithiothreitol, and 0.5 μg poly(dI-dC). The mixture was incubated at room temperature for 20 min and followed by separation on a 6% native polyacrylamide gel. After electrophoresis, the FAM signal was detected using a Typhoon Scanner (GE Healthcare). The probe sequences are listed in Table S2.

Promoter transient assay

The promoter transient assays were conducted as described previously with minor modifications (11). Briefly, TNG67 rice protoplasts were cotransformed with the effector, reporter, and internal control plasmids at a mass ratio of 1:1:0.5. After incubation, the protoplasts were collected and analyzed using the Dual-Luciferase Reporter Assay System (Promega) and the Cytation 5 cell imaging multimode reader equipped with a dual-reagent injector (BioTek).

Acknowledgments

This work was supported by funding from Academia Sinica, Taiwan. We acknowledge Professor Stanton Gelvin, Purdue University, for kindly providing the plasmid. We thank the Plant Tech Core Laboratory and the AS-BSCT greenhouse core facility of the Agricultural Biotechnology Research Center (ABRC), Academia Sinica, for technical support.

Supplementary material

Supplementary material is available at *PNAS Nexus* online.

Funding

This work was partially supported by the National Science and Technology Council (NSTC 111-2311-B-001-009 to M.-C.H.).

Author contributions

M.-C.S., M.-C.H., C.-C.L., and W.-J.L. conceived and designed the experiments, analyzed the data, and wrote the manuscript. C.-C.L., W.-J.L., C.-Y.Z., M.-Y.C., and C.-S.L. performed the experiments. T.-J.L. did recombinant protein expression and purification.

Data availability

All data are included in the manuscript and/or supporting information.

References

1 Xu K, *et al.* 2006. Sub1A is an ethylene-response-factor-like gene that confers submergence tolerance to rice. *Nature*. 442:705–708.
2 Fukao T, Xu K, Ronald PC, Bailey-Serres J. 2006. A variable cluster of ethylene response factor-like genes regulates metabolic and developmental acclimation responses to submergence in rice. *Plant Cell*. 18:2021–2034.
3 Fukao T, Bailey-Serres J. 2008. Submergence tolerance conferred by Sub1A is mediated by SLR1 and SLRL1 restriction of gibberellin responses in rice. *Proc Natl Acad Sci U S A*. 105:16814–16819.
4 Schmitz AJ, Folsom JJ, Jikamaru Y, Ronald P, Walia H. 2013. SUB1A-mediated Submergence tolerance response in rice involves differential regulation of the brassinosteroid pathway. *New Phytol*. 198:1060–1070.
5 Mustroph A, *et al.* 2010. Cross-kingdom comparison of transcriptomic adjustments to low-oxygen stress highlights conserved and plant-specific responses. *Plant Physiol*. 152:1484–1500.
6 Jung KH, *et al.* 2010. The submergence tolerance regulator Sub1A mediates stress-responsive expression of AP2/ERF transcription factors. *Plant Physiol*. 152:1674–1692.
7 Fukao T, Yeung E, Bailey-Serres J. 2012. The submergence tolerance gene SUB1A delays leaf senescence under prolonged darkness through hormonal regulation in rice. *Plant Physiol*. 160: 1795–1807.
8 Locke AM, Barding GA Jr, Sathnur S, Larive CK, Bailey-Serres J. 2018. Rice SUB1A constrains remodelling of the transcriptome and metabolome during submergence to facilitate post-submergence recovery. *Plant Cell Environ*. 41:721–736.
9 Gibbs DJ, *et al.* 2011. Homeostatic response to hypoxia is regulated by the N-end rule pathway in plants. *Nature*. 479:415–418.
10 Licausi F, *et al.* 2011. Oxygen sensing in plants is mediated by an N-end rule pathway for protein destabilization. *Nature*. 479: 419–422.
11 Lin CC, *et al.* 2019. Regulatory cascade involving transcriptional and N-end rule pathways in rice under submergence. *Proc Natl Acad Sci U S A*. 116:3300–3309.
12 Singh P, Sinha AK. 2016. A positive feedback loop governed by SUB1A1 interaction with MITOGEN-ACTIVATED PROTEIN KINASE3 imparts submergence tolerance in rice. *Plant Cell*. 28: 1127–1143.
13 Klemm SL, Shipony Z, Greenleaf WJ. 2019. Chromatin accessibility and the regulatory epigenome. *Nat Rev Genet*. 20:207–220.
14 Gates LA, Foulds CE, O'Malley BW. 2017. Histone marks in the 'driver's seat': functional roles in steering the transcription cycle. *Trends Biochem Sci*. 42:977–989.
15 Kim JM, *et al.* 2008. Alterations of lysine modifications on the histone H3 N-tail under drought stress conditions in *Arabidopsis thaliana*. *Plant Cell Physiol*. 49:1580–1588.
16 Zhou S, *et al.* 2017. Rice homeodomain protein WOX11 recruits a histone acetyltransferase complex to establish programs of cell proliferation of crown root meristem. *Plant Cell*. 29:1088–1104.
17 Li W, *et al.* 2011. DNA methylation and histone modifications regulate de novo shoot regeneration in Arabidopsis by modulating WUSCHEL expression and auxin signaling. *PLoS Genet*. 7: e1002243.
18 Li S, *et al.* 2019. The AREB1 transcription factor influences histone acetylation to regulate drought responses and tolerance in *Populus trichocarpa*. *Plant Cell*. 31:663–686.
19 Lee TA, Bailey-Serres J. 2019. Integrative analysis from the epigenome to translatome uncovers patterns of dominant nuclear regulation during transient stress. *Plant Cell*. 31:2573–2595.
20 Tsuji H, Saika H, Tsutsumi N, Hirai A, Nakazono M. 2006. Dynamic and reversible changes in histone H3-Lys4 methylation and H3 acetylation occurring at submergence-inducible genes in rice. *Plant Cell Physiol*. 47:995–1003.
21 Weake VM, Workman JL. 2012. SAGA function in tissue-specific gene expression. *Trends Cell Biol*. 22:177–184.
22 Balasubramanian R, Pray-Grant MG, Selleck W, Grant PA, Tan S. 2002. Role of the Ada2 and Ada3 transcriptional coactivators in histone acetylation. *J Biol Chem*. 277:7989–7995.
23 Sterner DE, Wang X, Bloom MH, Simon GM, Berger SL. 2002. The SANT domain of Ada2 is required for normal acetylation of histones by the yeast SAGA complex. *J Biol Chem*. 277:8178–8186.
24 Moraga F, Aquea F. 2015. Composition of the SAGA complex in plants and its role in controlling gene expression in response to abiotic stresses. *Front Plant Sci*. 6:865.
25 Vlachonasios KE, Thomashow MF, Triezenberg SJ. 2003. Disruption mutations of ADA2b and GCN5 transcriptional adaptor genes dramatically affect Arabidopsis growth, development, and gene expression. *Plant Cell*. 15:626–638.
26 Hark AT, *et al.* 2009. Two Arabidopsis orthologs of the transcriptional coactivator ADA2 have distinct biological functions. *Biochim Biophys Acta*. 1789:117–124.
27 Kotak J, *et al.* 2018. The histone acetyltransferase GCN5 and the transcriptional coactivator ADA2b affect leaf development and trichome morphogenesis in Arabidopsis. *Planta*. 248:613–628.
28 Mao Y, Pavangadkar KA, Thomashow MF, Triezenberg SJ. 2006. Physical and functional interactions of Arabidopsis ADA2 transcriptional coactivator proteins with the acetyltransferase GCN5 and with the cold-induced transcription factor CBF1. *Biochim Biophys Acta*. 1759:69–79.
29 Weiste C, Dröge-Laser W. 2014. The Arabidopsis transcription factor bZIP11 activates auxin-mediated transcription by recruiting the histone acetylation machinery. *Nat Commun*. 5:3883.
30 Seo YS, *et al.* 2011. Towards establishment of a rice stress response interactome. *PLoS Genet*. 7:e1002020.
31 Boyer LA, *et al.* 2002. Essential role for the SANT domain in the functioning of multiple chromatin remodeling enzymes. *Mol Cell*. 10:935–942.
32 Boyer LA, Latek RR, Peterson CL. 2004. The SANT domain: a unique histone-tail-binding module. *Mol Cell Biol*. 5:158–163.
33 Lee LY, Fang MJ, Kuang LY, Gelvin SB. 2008. Vectors for multi-color bimolecular fluorescence complementation to investigate protein-protein interactions in living plant cells. *Plant Methods*. 4:24.
34 Gamper AM, Kim J, Roeder RG. 2009. The STAGA subunit ADA2b is an important regulator of human GCN5 catalysis. *Mol Cell Biol*. 29:266–280.
35 Vamos EE, Boros IM. 2012. The C-terminal domains of ADA2 proteins determine selective incorporation into GCN5-containing

complexes that target histone H3 or H4 for acetylation. *FEBS Lett*. 586:3279–3286.
36 Sun J, *et al*. 2018. Structural basis for activation of SAGA histone acetyltransferase Gcn5 by partner subunit Ada2. *Proc Natl Acad Sci U S A*. 115:10010–10015.
37 Hoke SM, Genereaux J, Liang G, Brandl CJ. 2008. A conserved central region of yeast Ada2 regulates the histone acetyltransferase activity of Gcn5 and interacts with phospholipids. *J Mol Biol*. 384: 743–755.
38 Jiang B, *et al*. 2011. Sodium sulfite is a potential hypoxia inducer that mimics hypoxic stress in *Caenorhabditis elegans*. *J Biol Inorg Chem*. 16:267–274.
39 Jitsuyama Y. 2013. Responses of Japanese soybeans to hypoxic condition at rhizosphere were different depending upon cultivars and ambient temperatures. *Am J Plant Sci*. 4:1297–1308.
40 Lu H, Gao Z, Zhao Z, Weng J, Ye J. 2016. Transient hypoxia reprograms differentiating adipocytes for enhanced insulin sensitivity and triglyceride accumulation. *Int J Obes (Lond)*. 40:121–128.
41 Marino KM, Silva ER, Windelborn JA. 2020. A comparison between chemical and gas hypoxia as models of global ischemia in zebrafish (*Danio rerio*). *Animal Model Exp Med*. 3:256–263.
42 Biel M, Kretsovali A, Karatzali E, Papamatheakis J, Giannis A. 2004. Design, synthesis, and biological evaluation of a small-molecule inhibitor of the histone acetyltransferase Gcn5. *Angew Chem Int Ed Engl*. 43:3974–3976.
43 Aquea F, Timmermann T, Herrera-Vásquez A. 2017. Chemical inhibition of the histone acetyltransferase activity in *Arabidopsis thaliana*. *Biochem Biophys Res Commun*. 483:664–668.
44 Rymen B, *et al*. 2019. Histone acetylation orchestrates wound-induced transcriptional activation and cellular reprogramming in Arabidopsis. *Commun Biol*. 2:404.
45 Parnell SC, *et al*. 2005. Phosphorylation of the RGS protein Sst2 by the MAP kinase Fus3 and use of Sst2 as a model to analyze determinants of substrate sequence specificity. *Biochemistry*. 44: 8159–8166.
46 Brinkworth RI, Munn AL, Kobe B. 2006. Protein kinases associated with the yeast phosphoproteome. *BMC Bioinformatics*. 7:47.
47 Winters MJ, Pryciak PM. 2018. Analysis of the thresholds for transcriptional activation by the yeast MAP kinases Fus3 and Kss1. *Mol Biol Cell*. 29:669–682.
48 Pearlman SM, Serber Z, Ferrell JE Jr. 2011. A mechanism for the evolution of phosphorylation sites. *Cell*. 147:934–946.
49 Hunter T. 2012. Why nature chose phosphate to modify proteins. *Philos Trans R Soc Lond B Biol Sci*. 367:2513–2516.
50 Candau R, Berger SL. 1996. Structural and functional analysis of yeast putative adaptors. Evidence for an adaptor complex in vivo. *J Biol Chem*. 271:5237–5245.
51 Zhou S, *et al*. 2017. Rice homeodomain protein WOX11 recruits a histone acetyltransferase complex to establish programs of cell proliferation of crown root meristem. *Plant Cell*. 29:1088–1104.
52 Gibney ER, Nolan CM. 2010. Epigenetics and gene expression. *Heredity (Edinb)*. 105:4–13.
53 Shi J, Dong A, Shen WH. 2014. Epigenetic regulation of rice flowering and reproduction. *Front Plant Sci*. 5:803.
54 Zhou Y, *et al*. 2022. Phosphatidic acid modulates MPK3- and MPK6-mediated hypoxia signaling in Arabidopsis. *Plant Cell*. 34: 889–909.
55 Chen J, *et al*. 2019. NPR1 promotes its own and target gene expression in plant defense by recruiting CDK8. *Plant Physiol*. 181: 289–304.
56 Singh S, Kailasam S, Lo JC, Yeh KC. 2021. Histone H3 lysine4 trimethylation-regulated GRF11 expression is essential for the iron-deficiency response in *Arabidopsis thaliana*. *New Phytol*. 230: 244–258.
57 Su J, *et al*. 2018. Active photosynthetic inhibition mediated by MPK3/MPK6 is critical to effector-triggered immunity. *PLoS Biol*. 16:e2004122.